UNIVERSITY OF CALIFORNIA
DEPARTMENT OF ENGINEERING
BERKELEY, CALIFORNIA

INSTITUTE OF ENGINEERING RESEARCH
AND
DIVISION OF ELECTRICAL ENGINEERING

ANTENNA LABORATORY

SUBJECT

"DIFFRACTION OF A PLANE ELECTRO-MAGNETIC WAVE BY A CIRCULAR APERTURE AND COMPLEMENTARY OBSTACLE, PART II - DISCUSSION OF EXPERIMENTAL RESULTS"

7
SERIES NO. .....
185
ISSUE NO. .....
SEPTEMBER 5, 1952
DATE .....

UNIVERSITY OF CALIFORNIA
DEPARTMENT OF ENGINEERING

ANTENNA LABORATORY

Issue No. 185

Report No. 17 on
Office of Naval Research
Contract N7onr-29529

DIFFRACTION OF A PLANE ELECTROMAGNETIC WAVE BY A CIRCULAR APERTURE AND COMPLEMENTARY OBSTACLE

PART II - DISCUSSION OF EXPERIMENTAL RESULTS

Prepared by: Samuel Silver
Samuel Silver, Professor of Engineering Science

Morris J. Ehrlich
Morris J. Ehrlich, Research Engineer

G. Held
G. Held, Research Engineer

Approved by: Thos. C. McFarland
T. C. McFarland, Director, Antenna Laboratory

Distribution:

Chief of Naval Research, Washington, D.C. (Code 427)	2
Naval Research Laboratory, (Code 2000)	9
Chief of Naval Research, (Code 460)	1
Naval Research Laboratory (Code 2020)	2
Naval Research Laboratory (Code 3480)	1
BuShips (Code 838D)	1
BuShips (Code 810)	1
Bureau of Ordnance (Re4f)	1
Bureau of Ordnance (AD3)	1
Bureau of Aeronautics (EL51)	1
Bureau of Aeronautics (EL1)	1
Chief of Naval Operations (Op-413)	1
Chief of Naval Operations (Op-20)	1
Chief of Naval Operations (Op-32)	1
Naval Air Development Station, Electronics Laboratory	1
O.N.R., New York	1
O.N.R., San Francisco	2
O.N.R., Boston, Massachusetts	1
O.N.R., Chicago, Illinois	1
O.N.R., Pasadena, California	1
Assistant Naval Attache for Research	2
Naval Ordnance Laboratory	1
U.S.N.E.L., San Diego, California	2
U.S. Naval Academy, Electrical Eng. Dept., Annapolis	1
Commandant Coast Guard (EEE)	1
Office of the Chief Signal Officer (SIGET)	1
Signal Corps Engineering Laboratories, Attn: Mr. Woodyard	1
Electronics Laboratory, Wright Field (MCREER)	1
AMC Watson Laboratories, Attn: Dr. P. Newman	1
AMC Cambridge Research Laboratory, Attn: Dr. Spencer	1
Headquarters, U.S. Air Force (AEMEN-2)	1
Research and Development Board, Washington, D.C.	1
National Bureau of Standards	1
Cruft Laboratory, Harvard University, Attn: Prof. King	1
Mass. Institute of Technology, Attn: Prof. L.J. Chu	1
Stanford University, Attn: Dean F.E. Terman	1
E.E. Department, Illinois University, Attn: Prof. Jordan	1
Ohio State University Research Foundation, Dr. Rumsey	1
E.E. Department, Cornell University, Attn: Dr. H.G. Booker	1
Stanford Research Institute, Attn: Dr. J.V.N. Granger	1
Polytechnic Institute of Brooklyn, Attn: Dr. A. Oliner	1
Washington Square College, N.Y.U. Math Group, Attn: Prof. Kline	1
Squier Signal Laboratory, Attn: Vicent J. Kublin	1

1. Introduction

This report, Part II of the series[8], is devoted to experimental studies of diffraction of electromagnetic waves by a circular aperture and to an evaluation of certain theoretical developments. All available theoretical results are fundamentally in the nature of approximations for the two extremes of the size of the aperture (or obstacle) relative to the wavelength, the very large and the very small. From the practical standpoint, however, the intermediate range is of greater interest and, therefore, the problem of closing the gap in the theoretical work is a very significant one. It is difficult to assess mathematically the range over which a given approximation will give good results, particularly in the application of the theory to the near-zone field structure.* One of the objects of the experimental study is to determine the usefulness of various theories for the near-zone field.

Our work was stimulated to a large degree by the results of an experimental study of the diffraction of a plane wave by a circular aperture in a large metal sheet which were published by C.L. Andrews[1] several years ago. Andrews measured the component of electric field intensity parallel to the sheet-which we designate as the tangential component - in the near-zone region up to and including the aperture itself. He observed large

---

*We are concerned primarily with the near-zone field. The theoretical situation is far better with respect to integrated properties such as transmission coefficients and aperture impedance. These have been dealt with quite successfully by H. Levine and J. Schwinger by variational techniques. See for example, Communications on Pure and Applied Mathematics, 3, 355: (1950)

fluctuations in field intensity across the aperture, the number of maxima and minima being directly related to the ratio of the diameter to the wavelength. He noted that the distribution of maxima and minima in the aperture and also along the axis normal to the aperture was accurately accounted for by the well known Fresnel zone concept used in optics and scalar diffraction problems. He also found that the scalar Kirchhoff theory gives a good semi-quantitative representation of the field structure. This is somewhat surprising for the range of aperture dimensions involved, the largest being of the order of six wavelengths.

In the present study the range of aperture dimensions was extended to 36λ. A question had been raised as to the possibility that the fluctuations in field intensity are the result of multiple scattering between the antenna used to explore the field and the metal sheet. We have examined this point quite carefully and are convinced that multiple scattering is responsible only for certain fine structure features of the pattern. In addition to having extended the range of the data on the tangential electrical field we have also obtained results for the other field components. The most important of these are the tangential magnetic field components which play an important part in an exact formulation of the theory and which are especially pertinent to the high frequency approximation which we presented in Part I.

The discussion and experimental results which are given in the following sections deal with the case of a linearly polarized plane wave incident normally on a plane sheet. The diffracting edge, whether that of an aperture in an extended metal

sheet or of the complementary disc, is a circle. The essential geometrical elements used in our discussion are shown in Fig. 1, which illustrates the situation of a circular aperture S_o in an otherwise infinite conducting surface S_m. For the purposes of theory the conducting sheet S_m is taken to have infinite conductivity and zero thickness.

The numerical evaluation of theoretical expressions for the near-zone field and measurements in this region are generally very laborious. The results obtained so far cover only the distributions along the axis and in the principal E- and H-planes. The latter are respectively the plane containing the incident electric vector and the one orthogonal to it.

A detailed discussion of experimental technique and sources of experimental error will be given in Part III. For the present, however, we should note that we made measurements both on a complete space system and on a half-space system. The half-space system makes use of the symmetry properties of the field with respect to the plane perpendicular to the electric vector of the incident wave. This symmetry plane can be replaced by an infinite perfectly conducting sheet without affecting the field in the half-spaces on either side. The ideal half-space situation is approximated by using a large ground plane with suitable absorbing walls at the edges to eliminate reflections. The half-space technique has the advantage that the major portion of the measurement apparatus is then below the ground plane out of the way of the field.

2. Small Apertures, Diameter $D \leq \lambda$; small hole theory.

Figures 2, 3 and 4 show some of the measured distributions of the tangential electric field for apertures of diameter $D = 0.5\lambda$ and $D = 1.0\lambda$. In both cases the axial distribution decreases monotonically from the aperture. This is readily understood in terms of the Fresnel zone concept. For any point on the axis the aperture subtends less than one Fresnel zone, that is, the contribution from any one element of the aperture is never 180° out of phase with that of any element and we do not have the possibility of strong destructive interference with the resulting minimum in the distribution as in the case of larger apertures.

It is interesting to compare the measurements with small hole theory. The case of an aperture whose dimensions are very small compared with the wavelength has been treated extensively to various degrees of approximation. The most satisfactory work is that of Bouwkamp[4]* who developed the correct first order expressions for a circular aperture which are valid both in the near-zone and far-zone region. For the case of the incident electric vector as shown in Fig. 1, Bouwkamp's results take the following form:

$$E_y = -jkz + j\frac{2ka u}{\pi}\left\{1 + v\tan^{-1}v + \frac{1}{3(u^2+v^2)} + \frac{y^2 - x^2}{3a^2(1+v^2)^2(u^2+v^2)}\right\} \qquad (1a)$$

$$E_x = \frac{j4kxyu}{3\pi a(u^2+v^2)(1+v^2)^2} \qquad E_z = \frac{-j4kyv}{3\pi(u^2+v^2)(1+v^2)} \qquad (1b)$$

where u, v are oblate spheroidal coodinates related to the cartesian

*We are indebted to Dr. Bouwkamp for having made his work available to us prior to its publication.

ecordinates by

$$x = a\left[(1-u^2)(1+v^2)\right]^{\frac{1}{2}} \cos\phi \qquad (2a)$$

$$z = a\left[(1-u^2)(1+v^2)\right]^{\frac{1}{2}} \sin\phi \qquad (2b)$$

$$z = auv \qquad (2c)$$

with $0 \leq u \leq 1$, $-\infty < v < \infty$, $0 \leq \phi \leq 2\pi$, $\underline{a}$ is the radius of the aperture and $k = \frac{2\pi}{\lambda}$

The above expressions are correct up to terms of relative order $(ka)^2$ and, therefore, may be expected to give good results for apertures of size such that

$$ka < 1 \quad \text{or} \quad a < \frac{\lambda}{6}$$

The two cases to which our figures apply, $a = \frac{\lambda}{4}$ and $a = \frac{\lambda}{2}$, are outside this range. However, it is observed that the small hole theory is still of semiquantitative value for these cases. The small hole theory predicts a larger value of intensity in the aperture itself than that which is observed but it does run close to the measured axial distribution outwards from a small distance beyond the aperture. Figure 3 shows the distribution in a plane parallel to the aperture for the $a = \frac{\lambda}{4}$ case. Only H-plane experimental data are shown. The E-plane data do not differ substantially. It will be noted that the small hole theory is inapplicable insofar as establishing the absolute level is concerned. But, as Fig. 3b shows, the theory serves well for the relative distribution. Similar results were found for the larger aperture ($a = 0.5\lambda$). When the radius exceeded 0.5λ no particularly meaningful connection between the small hole theory and the experimental results could be observed. The small hole theory necessarily

loses significance when the aperture contains more than one Fresnel zone.

3. Tangential Field Components in the Aperture; $D \geq \lambda$

When the diameter of the aperture is greater than one wavelength, the near-zone field pattern is marked by fluctuations in the magnitudes of the field vectors. The pattern of the tangential components in the aperture itself is of particular interest to us in connection with the development of an adequate theoretical solution. It was pointed out by Andrews that for the tangential electric field the interference pattern is most marked in the aperture itself. Similar observations were made by Severin[7] who also measured the electric field in the near zone. Our data, shown in Figs. 5 - 9 inclusive, are in good agreement with those of Andrews and Severin and confirm the previously observed complexity of the field structure.

It is observed that the H-plane pattern shows more variation in structure than the E-plane pattern. Up to an aperture diameter of 16λ there appears to be a systematic relationship between the number of maxima and minima and the size of the aperture. When the aperture diameter $D = n\lambda$, n being an integer, the number of maxima in the H-plane pattern is equal to n. When n is even, the pattern has a minimum at the center of the aperture; when n is odd, the pattern has a maximum at the center. This type of relationship can be visualized in terms of a standing wave in the aperture associated with the boundary condition that at the edge the component of $\vec{E}$ which is tangential to the edge vanishes. The behavior of the field at the center can also be

correlated with the number of Fresnel zones subtended by the aperture, in a limited sense, at the center.

The preciseness of the relationship stated above may be questioned on the basis of Fig. 7 which shows the H-plane pattern for the case of D = 36λ. The latter differs from the smaller apertures not only with respect to the number of maxima and minima, but also in the detailed form of the pattern. In the smaller apertures the maxima and minima are relatively uniform in size whereas in the large aperture there is considerable variation in size of a form suggestive of modulation by another distribution function of longer space periodicity. A trend toward this latter structure is observable in the pattern of the 16λ aperture. Unfortunately we do not have data for cases intermediate between 16λ and 36λ. It will be worthwhile to make further studies to fill in the gap. The change in structure is perhaps connected with the phase error in the incident field which developes with increased aperture size. In our experimental work the primary source is a horn placed sufficiently far from the aperture plane so that the latter is in its far zone field. The aperture is, therefore, being illuminated by a spherical wave. With the distance from the horn to the aperture plane being held fixed, the deviation from constant phase increases with the increasing aperture size. In addition, the amplitude distribution changes because of the primary pattern of the horn; the incident field amplitude becomes increasingly tapered as the aperture becomes larger. Both factors profoundly modify the pattern from that which would be produced by an ideal plane wave. The effect of

amplitude taper was investigated by Sterns[10] in a study of the near-zone field of paraboloidal reflectors. It should also be noted that the large apertures are only nominally an integral number of wavelengths in diameter.

The distribution of E_{tan} in the aperture is, of course, dependent on conditions all around the edge, not merely at any two special points. The behavior of the field at the edge has been the subject of much discussion over the past few years. Bouwkamp[5] called attention to the role of singularities in diffraction theory and on the basis of the Sommerfeld solution[9] for the half-plane, postulated certain edge conditions for the general aperture case. These edge conditions were developed in greater detail by Meixner[6] and others. If we let E_τ and E_n' be the components of E_{tan} which are respectively tangential and normal to the edge of the aperture, the edge conditions are that

$$E_\tau = 0 \tag{3a}$$

and that the singularity of E_n' is at best

$$E_n' \simeq \frac{1}{r^{\frac{1}{2}}} \tag{3b}$$

where r is the distance along n' from the edge of the aperture. These conditions assume that the screen is infinitely conducting and is of zero thickness. The first, (3a), is the logical extension of the condition that the tangential component of $\bar{E}$ must vanish over the screen. The second condition is a statement that the energy density at the edge is integrable.

The boundary condition (3a) shows up nicely in the

experimental H-plane patterns. It is observed in each case of Fig. 6, with the exception of that of D = 6λ, and in Fig. 7, that the intensity drops sharply at the edge of the aperture. With respect to boundary condition (3b), on the other hand, the results are completely non-definitive. Singularities, if there are any, should be most evident in the E-plane pattern. A careful examination of the field to detect a sharp rise near the edge gave negative results. There are several factors which limit the reliability of the data: The sheet has a finite thickness; this factor was reduced by filing the aperture boundary to a sharp edge. The resolution that can be obtained in a field measurement is limited by the finite extent of the probe; there is a practical limit to which the probe and the supporting structure can be reduced. Then there is the interaction between the probe and the screen which becomes particularly significant at points where the field intensity is high. Because of the latter two factors, the E-plane pattern, in general, is more subject to experimental error than the H-plane pattern. By use of the half-space technique the errors are reduced to a considerable extent in the H-plane pattern. In the case of the E-plane measurements, however, there are further difficulties with the half-space technique generated by interaction between the probe and its image.

The field structure shown in Fig. 7 is at variance with the ideas generally entertained about large apertures. The argument is frequently set forth that, on physical grounds, one should expect the field in the aperture to approach the unperturbed incident field with increasing aperture size, the diffraction

effects becoming limited to small regions in the neighborhood of the edge. This view is also suggested by the argument that when the radius of the aperture is large, the diffraction problem for any small section of the edge is locally the same as that of diffraction of a plane wave by a straight edge. It is apparent, however, that the height of the central maximum in Fig. 7 is not appreciably different from that observed in the smaller apertures. If we think of the edge as forming a distribution of sources of diffraction wavelets, then with the circular geometry, these wavelets are all in phase at center. Hence, although each component wavelet amplitude may be small, the sum total is large and is essentially independent of the aperture radius. The phase of the resultant with respect to the incident plane wave is a function of the radius and consequently there occurs a maximum or minimum at the center according to the dimensions of the aperture. Further work on different aperture geometry will aid in understanding what does take place.

The behavior of H_{tan} in the aperture is radically different from that of E_{tan}. The rigorous formulation of the diffraction problem and the application of the fundamental boundary conditions in the aperture directly establishes that H_{tan} in the aperture is the same as that of the unperturbed plane wave. In the case of normal incidence H_{tan} should, therefore, be constant over the aperture. This property shows up beautifully in the experimental H_{tan} patterns shown in Fig. 10. In the $D = 1\lambda$ case the apparent deviation from the theoretical result is again the

cause of limited resolving power and interaction between the probe and the screen. The probe used for these measurements was a slot antenna flush mounted in the ground plane. It is seen that at the edge of the aperture H_{tan} drops sharply to virtually zero. This behavior of H_{tan} forms the experimental basis for the high-frequency development given in Part I.

4. Complementary Obstacle - Tangential Components

It is interesting to compare the diffraction field of an aperture with that of the complementary obstacle. Fig. 11 shows typical field patterns of E_{tan} and H_{tan} in the H-plane for the complementary obstacles of diameters 3λ and 5λ. The behavior of E_{tan} outside the disc boundary is very much like that of the diffraction field of a straight edge given by the Sommerfeld theory. The amplitude of oscillation diminishes with increasing distance from the edge and the field approaches the unperturbed field value. The field structure can also be interpreted from the point of view that the diffraction effects arise from secondary wavelets generated at the edge of the disc.

H_{tan} exhibits the constant value over the open area predicted by the rigorous theory. It is observed that the field amplitude drops sharply at the edge of the disc and is virtually zero over the shadow region. This means that the perturbation currents are confined to the neighborhood of the boundary and that over the illuminated side of the disc the current distribution is essentially that which would exist over the corresponding area in reflection of the plane wave from an infinite screen. It

will be noted that there is a peak in the H_{1a} distribution at the center of the disc on the shadow side. This will recall the familiar bright spot observed on the axis in the diffraction pattern of a circular object in the optical region. The Fresnel zone interpretation of the effect is well-known.

One of the important theoretical results concerning diffraction by apertures and complementary sheet obstacles is the electromagnetic Babinet principle which was formulated by Booker[3]. The principle is as follows: Suppose that we have a field $\vec{E}_{1a}$, $\vec{H}_{1a}$ incident on an aperture and that $\vec{E}_1$, $\vec{H}_1$ is the diffraction field in the region $z > 0$; then, if in the case of a complementary obstacle we have an incident field

$$\left.\begin{aligned} \vec{E}_{1b} &= -\left(\frac{\mu}{\epsilon}\right)^{\frac{1}{2}} \vec{H}_{1a} \\ \vec{H}_{1b} &= \left(\frac{\epsilon}{\mu}\right)^{\frac{1}{2}} \vec{E}_{1a} \end{aligned}\right\} \qquad (4)$$

and $\vec{E}_2$, $\vec{H}_2$ is the corresponding diffraction field, the two diffraction fields satisfy the relation

$$\vec{E}_1 + \left(\frac{\mu}{\epsilon}\right)^{\frac{1}{2}} \vec{H}_2 = \vec{E}_{1a} \qquad (5a)$$

$$\vec{H}_1 - \left(\frac{\epsilon}{\mu}\right)^{\frac{1}{2}} \vec{E}_2 = \vec{H}_{1a} \qquad (5b)$$

The principle is a result of the exact theory and as such provides a way to check the reliability of the experimental technique. Fig. 12 shows the results of measurements of complementary fields along a line parallel to the aperture plane. Since the field components

are normalized to the incident field values, the result of the superposition according to Eq. (5a) should be unity. It is seen that the sum lies close to unity over the entire range of the measurement. The deviations are within the estimated errors of the measurements. The best mean line through the sum data shows a downward trend across the line of measurement. This may represent the tapered illumination corresponding to the primary pattern of the horn but it is questionable whether the data are sufficiently reliable to reproduce the incident field so exactly.

5. Axial Distribution - Apertures, $D \geq \lambda$

The axial distributions of E_{tan} and H_{tan} for a sequence of aperture sizes are shown in Fig. 13. It is observed that in each case H_{tan} approaches unity as $z \to 0$, in agreement with the boundary condition on H_{tan} stated previously. Both E_{tan} and H_{tan} show the fluctuations in amplitude that are characteristic of the near-zone field. The two components are not in phase, however, as in a plane wave. This is indicated by the difference in the location of the maxima and minima. The two components approach one another with increasing distance from the aperture and finally do, of course, become related as in a plane wave when the far zone is reached. As was pointed out by Andrews, the location of the maxima and minima of the E_{tan} distribution are accounted for quite accurately by simple Fresnel zone considerations, particularly for the smaller apertures. The deviations from the Fresnel zone values increase with increasing aperture size. According to the Fresnel zone analysis there should be a minimum at $z = 0$ when the aperture diameter is an even number

of wavelengths. The field does in fact exhibit this property up to the aperture diameter of 6λ. However, it is seen in Fig. 13 that in the case of the 10λ aperture the minimum occurs somewhat beyond the aperture. It was thought that it could be due to the aperture not being precisely 10λ in diameter. The data shown in Fig. 13 were taken at X-band. Further measurements were made at K-band and the frequency was varied through the 10λ value for the aperture under study. The K-band data are in excellent agreement with those shown in Fig. 13. It was verified that the minimum is displaced from the center in the 10λ case. Our feeling now is that the effect is due to phase errors in the incident field.

6. Theoretical Considerations - High Frequency Approximations

All high frequency approximations, that is, for the case $D >> \lambda$, start from assumptions as to the boundary conditions over the aperture and the screen. They are not asymptotic developments of an exact theoretical solution. The two well known approximate solutions are the Kirchhoff theory for scalar waves and the modification of the scalar form by Kottler and others to fit the electromagnetic field equations. A discussion of these will be found in Baker and Copson's book[2]; a more recent development of Kottler's theory has been given by Stratton[11].

The experimental basis for the theories is the fact that as the aperture increases in size the diffraction field drops off rapidly as we pass into the shadow region. The tangential components of both $\vec{E}$ and $\vec{H}$ are, therefore, taken to be zero over the screen. The condition is, of course, rigorous insofar as $\vec{E}$

is concerned. It is further argued that when the aperture is large, the field in the aperture is very closely the same as the unperturbed field and the unperturbed field values are, therefore, taken as the boundary values of both $\vec{E}$ and $\vec{H}$ over the aperture area. As we have seen, this is a rigorous condition for H_{tan} in the aperture. For either of the Kirchhoff theories it is necessary to make assumptions about <u>both</u> E_{tan} and H_{tan} over the boundary plane $z = 0$. This is one of the major objections to the theories, namely, that the boundary conditions are over-prescribed, for in addition to the assigned values over $z = 0$ the field is required to satisfy radiation conditions at infinity. Either E_{tan} or H_{tan} alone over the plane $z = 0$, together with the radiation conditions, suffices to define the electromagnetic field problem. It turns out that the assumed boundary conditions on E_{tan} are not consistent with those assumed for H_{tan}.

The Kirchhoff theory gives identical field patterns for the electric and magnetic vectors. When the field expressions are extrapolated to the boundary surface $z = 0$ neither the assumed E_{tan} distribution nor H_{tan} distribution is obtained. Both field components have an oscillatory structure in the aperture such as is exhibited by the experimental E_{tan}. The theory also gives non-zero field values over the screen, values which do fall off rapidly from the edge. Neglecting the latter, we may state that the Kirchhoff theory gives fairly good results for the near-zone field structure of E_{tan}, but is seriously in error in its solution for H_{tan}.

The experimental results shown in Fig. 10 constitute

the basis for the high-frequency development given by us in Part I of this series. The assigned value of H_{tan} over the aperture is exact but, as in the Kirchhoff theory, we neglect the contribution of H_{tan} over the screen. However, boundary values are assigned only to H_{tan} and we have a clearly defined electromagnetic problem. Our procedure for solving the boundary value problem disguises the contributions of the electric charge distribution along the aperture boundary which must be associated with the discontinuous H_{tan} distribution. However, the contribution is contained within the solution and the latter satisfies Maxwell's equations. As the solution is developed, we are assured that it assumes the assigned values of H_{tan} over the plane $z = 0$. It does generate E_{tan} over the screen within a small region about the edge and in this respect is in error just as the Kirchhoff theories.

The various solutions require considerable numerical work in order to obtain the complete near-zone field. The calculations are in progress and results will be published as they become available. At the present time we have several axial distributions and Figs. 14 - 17 show comparisons between the Kirchhoff theory and the H_{tan} approximation and experimental results. For reference the expressions for the axial distributions obtained from the several theories are given below. In these expressions:

E_o, H_o = amplitudes of the vectors in the incident plane wave

a = radius of the aperture

$r_1 = \sqrt{a^2 + z^2}$.

The subscripts x, y refer to the directions of the vectors in terms of the axes shown in Fig. 1.

(a) Kirchhoff scalar theory:

$$\frac{E_y}{E_o} = -\frac{H_x}{H_o} = e^{-jks} - \frac{1}{2}\left[1 + \frac{z}{r_1}\right]e^{-jkr_1} \qquad (6)$$

(b) Victor Kirchhoff theory:

$$\frac{E_y}{E_o} = -\frac{H_x}{H_o} = e^{-jks} - \frac{1}{2}\left[1 + \frac{z}{r_1}\right]e^{-jkr_1}$$

$$+ \frac{1}{4}\left(\frac{a}{r_1}\right)^2\left(1 + \frac{1}{jkr_1}\right)e^{-jkr_1} \qquad (7)$$

(c) H_{tan} approximation*:

$$\frac{H_x}{H_o} = -e^{-jks} + \frac{z}{r_1}e^{-jkr_1} \qquad (8a)$$

$$\frac{E_y}{E_o} = e^{-jks} - e^{-jkr_1} + \frac{1}{2}\left(\frac{a}{r_1}\right)^2\left[1 + \frac{1}{jkr_1}\right]e^{-jkr_1} \qquad (8b)$$

It is seen in Figs. 14 - 16 that the Kirchhoff scalar solution gives essentially the same result as the H_{tan} approximation for the distribution of E_{tan}. The positions of the maxima and minima are almost identical. However, the Kirchhoff solution gives higher maxima and deeper minima. The solutions given by the two theories approach one another more closely as $\frac{D}{\lambda}$ increases. Fig. 16 is on

*C. J. Bouwkamp called our attention to the fact that the solutions given in Part I can be put into this form for the axial distribution.

an expanded scale to show the difference between them. As is seen in Figs. 14 and 15 the H_{tan} approximation gives the correct behavior of the H_{tan} distribution in the neighborhood of the aperture, but as the distance from the aperture increases the agreement between theory and experiment is only qualitative.

From physical considerations we would expect the H_{tan} approximation to become more satisfactory as $\frac{D}{\lambda}$ increases. The disagreement between theory and experiment manifested by the data shown in Fig. 17 is, therefore, quite surprising. However, on consideration of the geometry of the experimental setup it is found that for the case of Fig. 17 the incident magnetic field is not constant in phase over the aperture but has a phase error distribution with a maximum error of $\frac{\lambda}{4}$ from uniform phase. The tapering of the illumination also becomes effective. Previous experience with phase errors and tapered illumination has been that the amplitudes of the variations are reduced by those factors and that the positions of the maxima and minima are displaced in the direction presented by the experimental data. When the calculations are completed the results of the modified solution taking phase error into account will be published.

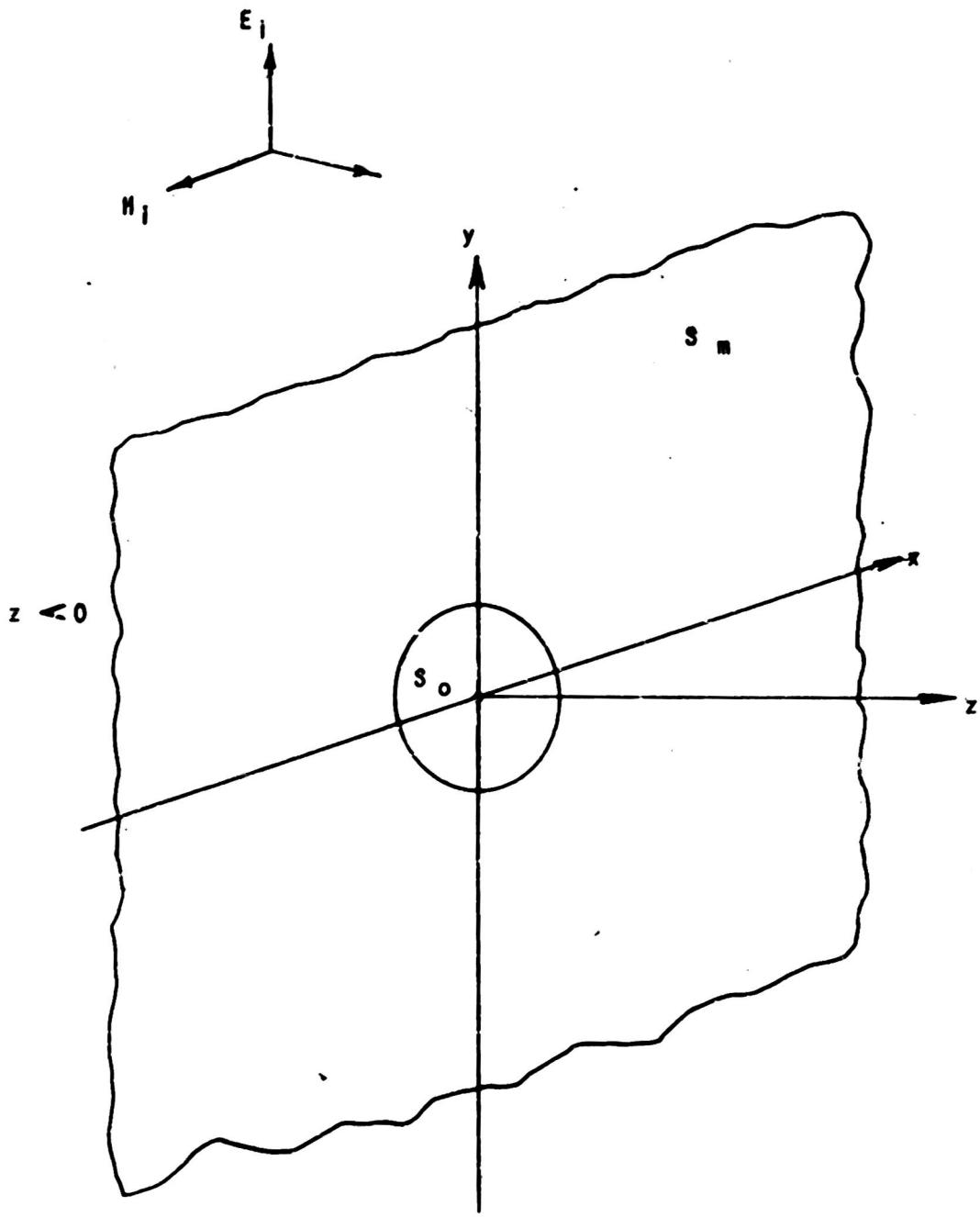

FIG 1

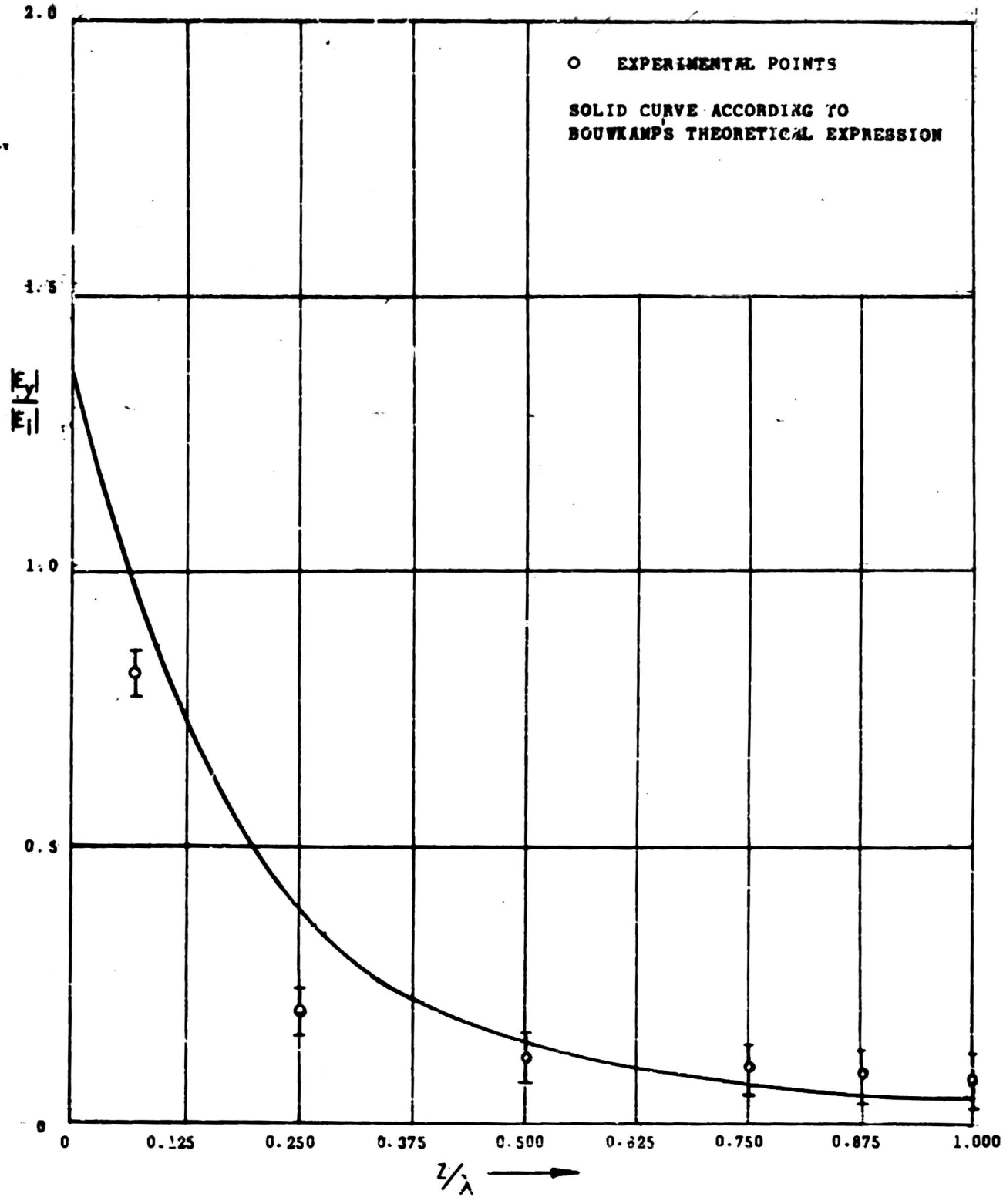

FIG. 2. TANGENTIAL ELECTRIC FIELD ALONG AXIS
APERTURE DIAMETER = 0.5 λ

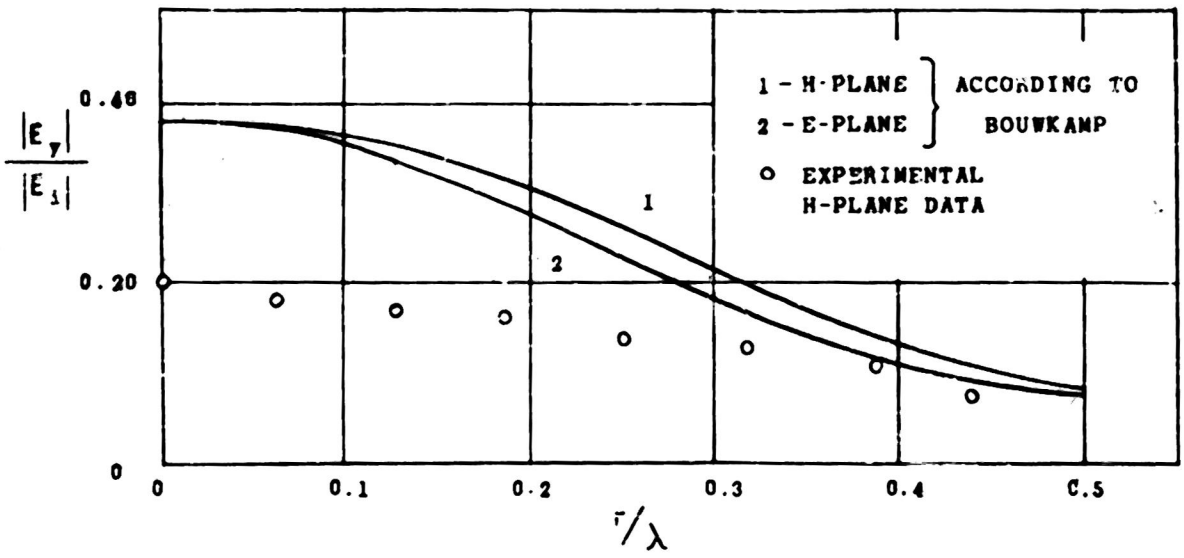

FIG 3a

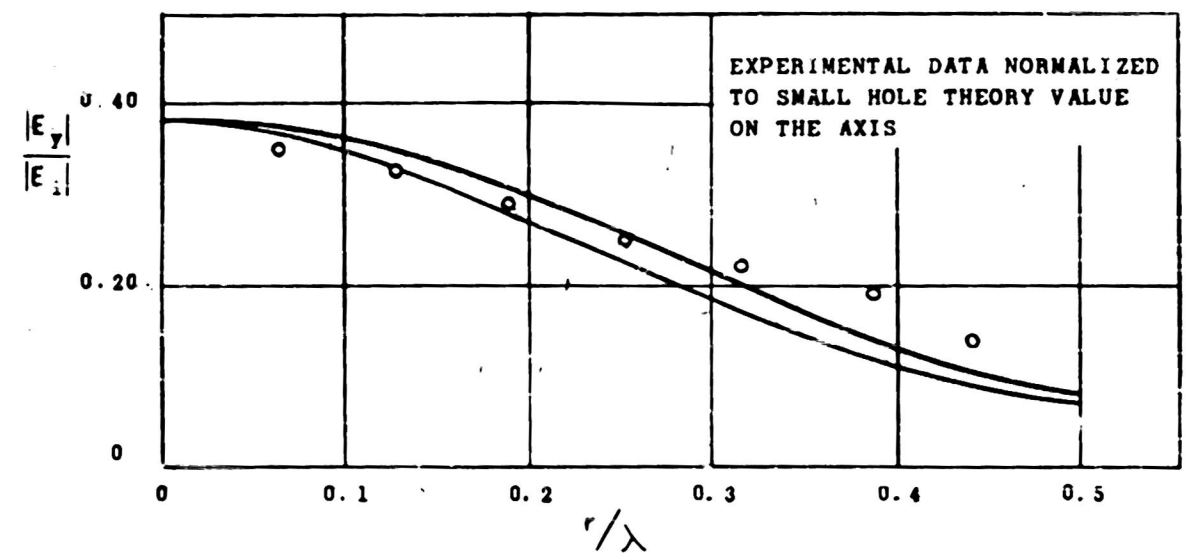

FIG 3b

FIG. 3 TANGENTIAL ELECTRIC FIELD ALONG A LINE PARALLEL TO AN APERATURE OF DIAMETER $D = 0.5\lambda$ AT A DISTANCE $Z = 0.25\lambda$

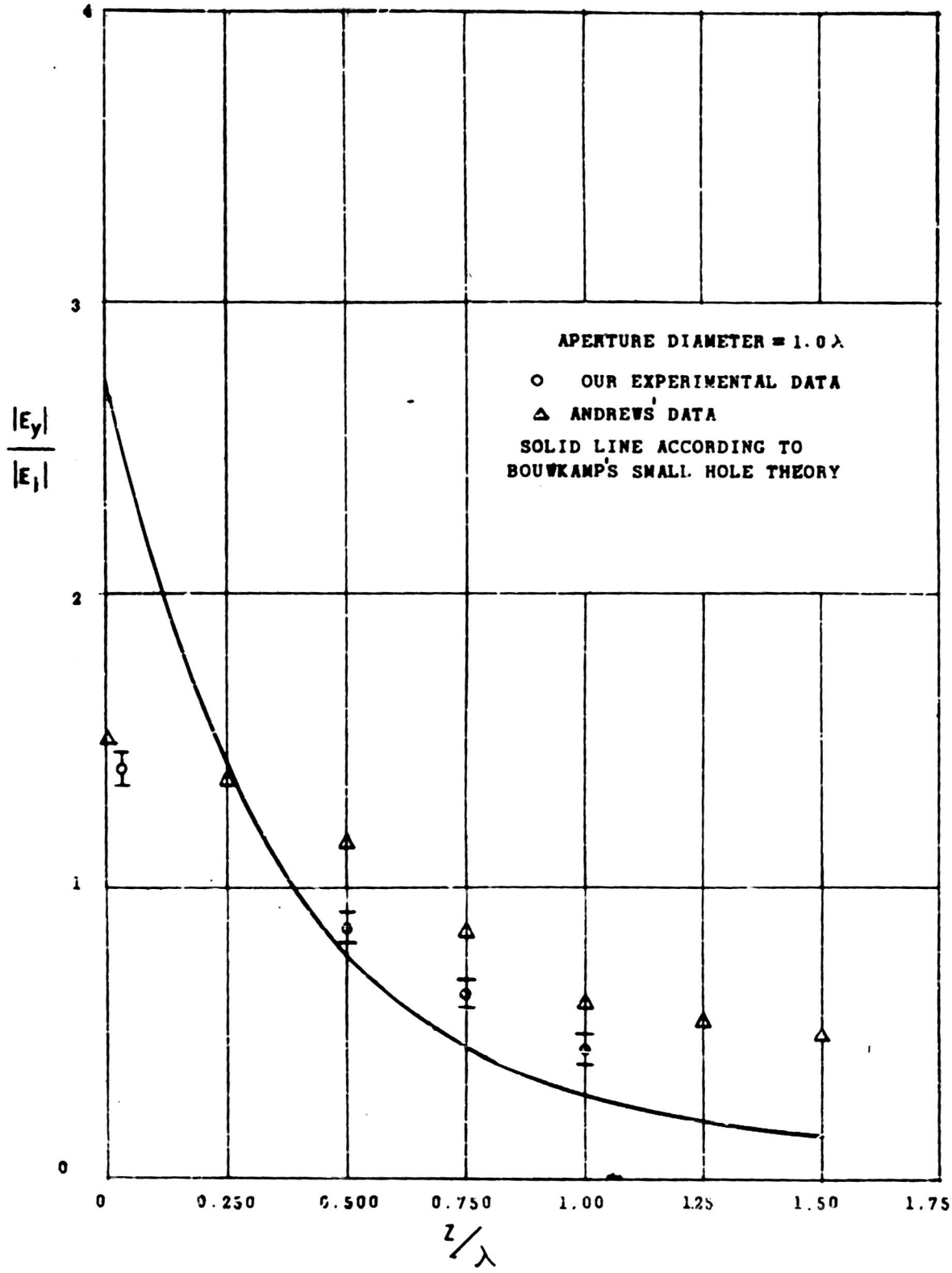

FIG. 4. AXIAL DISTRIBUTION OF THE TANGENTIAL ELECTRIC FIELD COMPONENT FOR AN APERTURE OF DIAMETER D = 1.0 λ

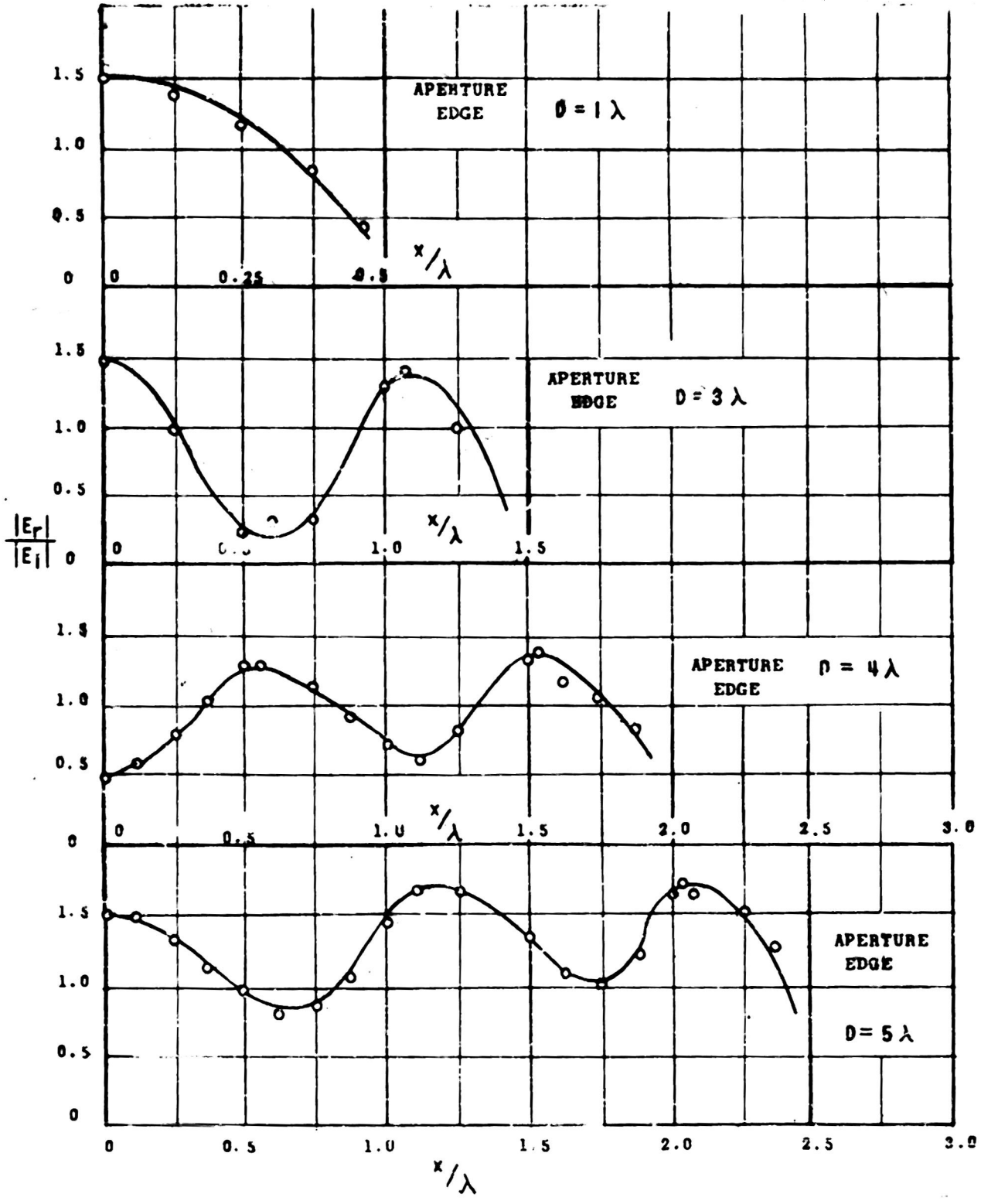

FIG. 5. E_T IN PLANE OF APERTURE NORMALIZED TO UNPERTURBED PLANE WAVE

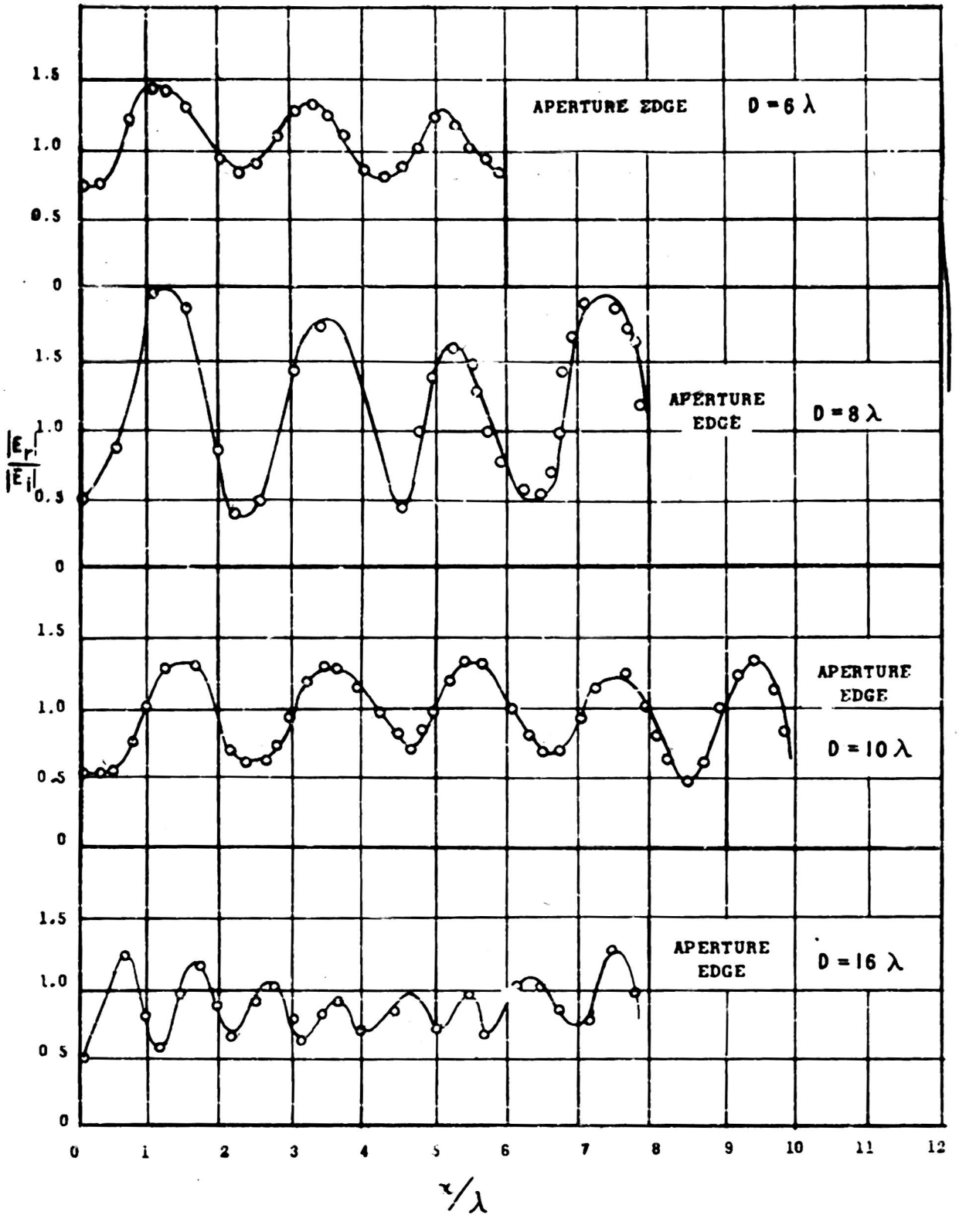

FIG. 6. E_T IN PLANE OF APERTURE

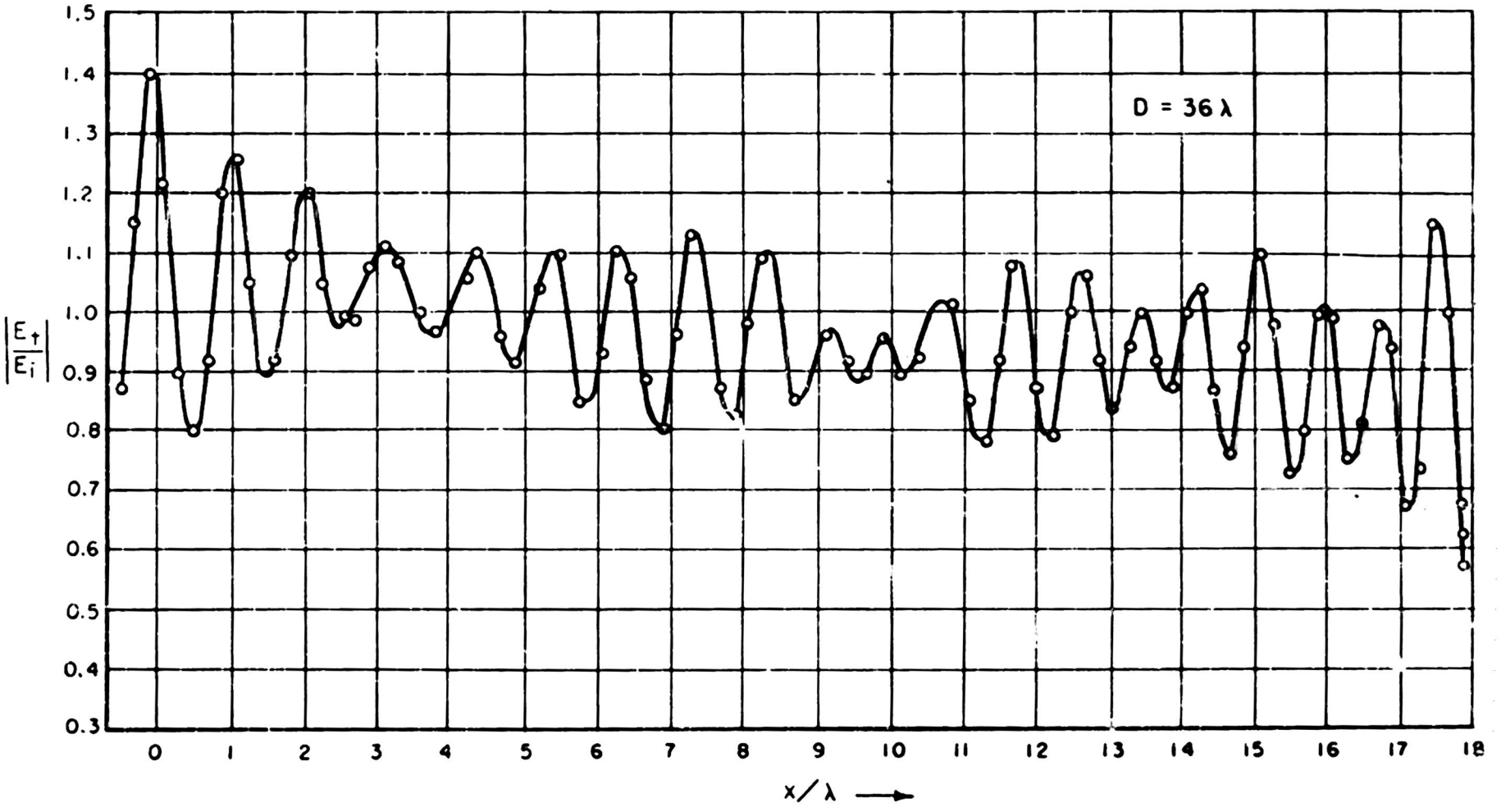

FIG 7 E_t IN THE PLANE OF THE APERTURE

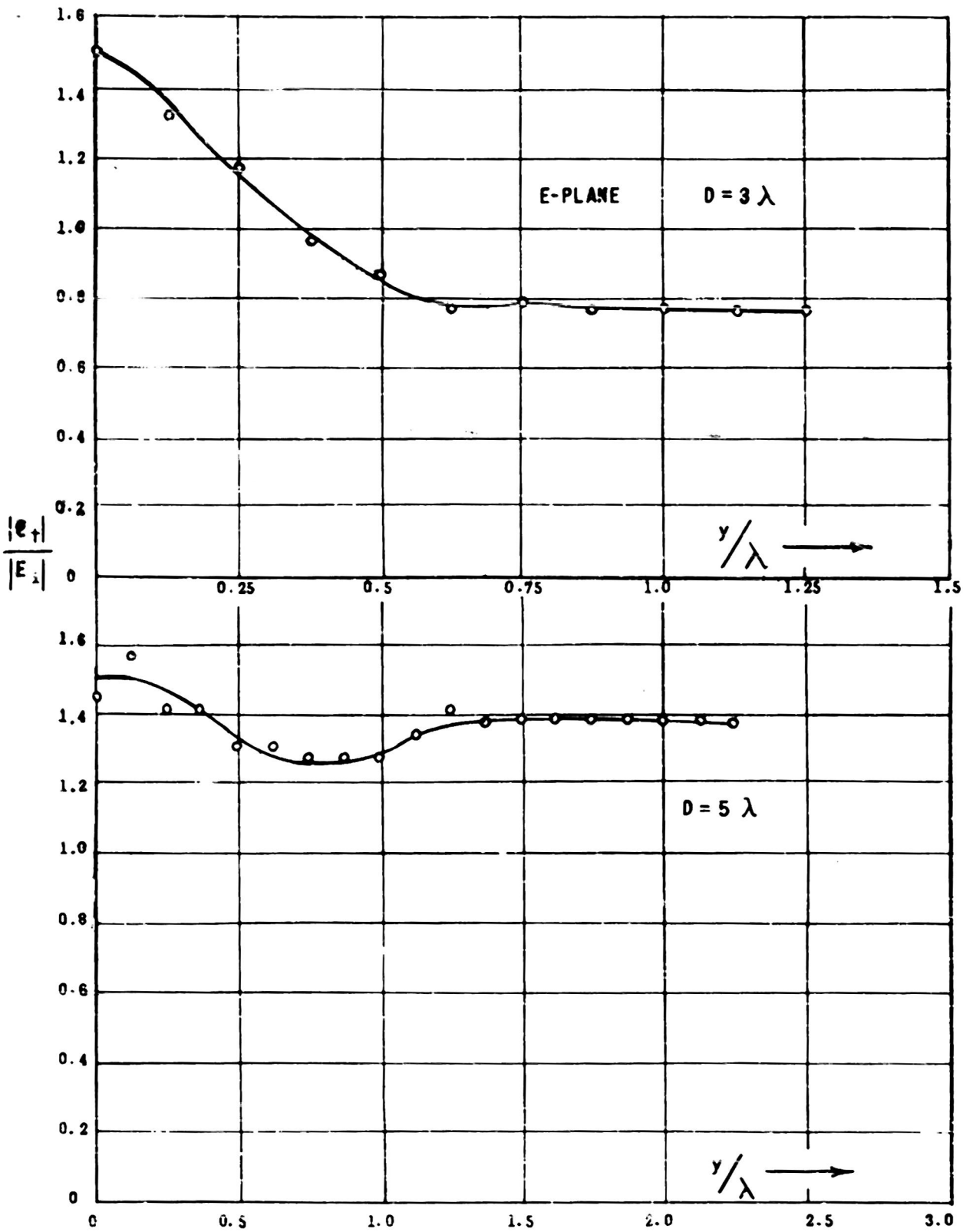

FIG. 8 TANGENTIAL ELECTRIC FIELD IN THE APERTURE; E-PLANE PATTERN

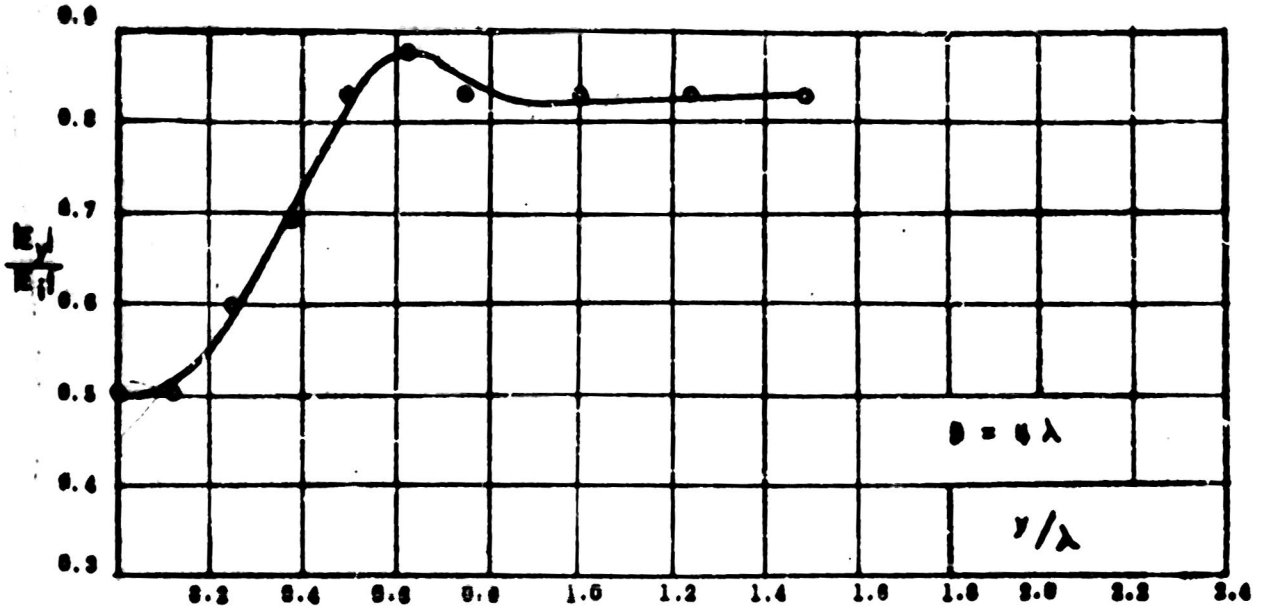

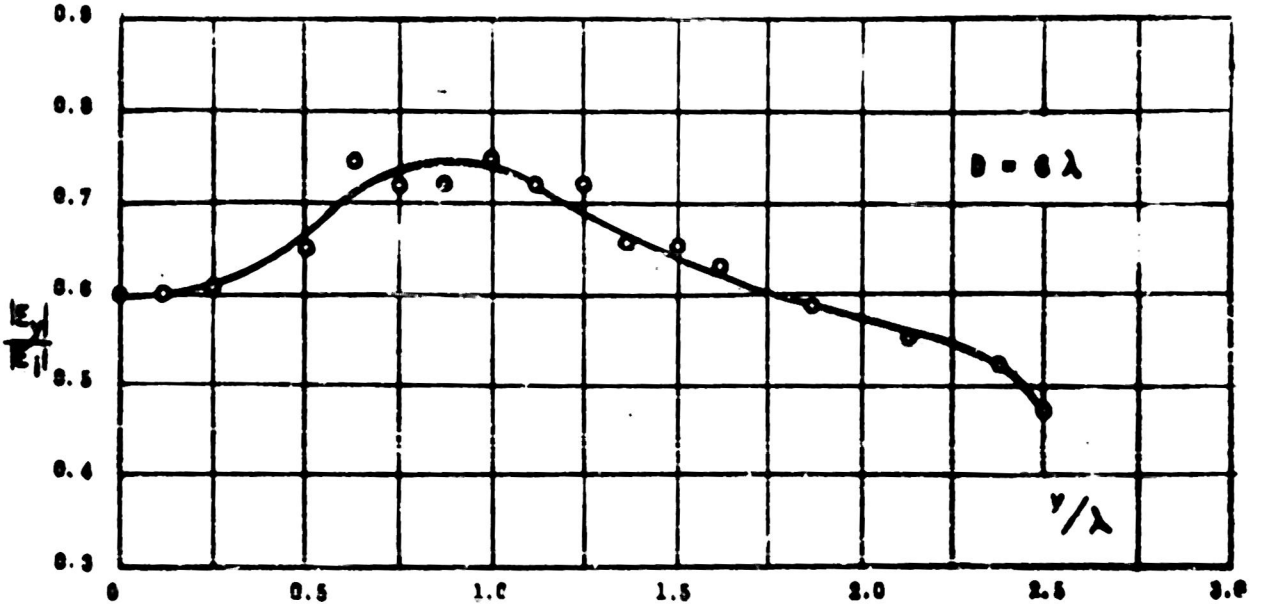

FIG.9 TANGENTIAL ELECTRIC FIELD IN THE APERTURE; E-PLANE PATTERN

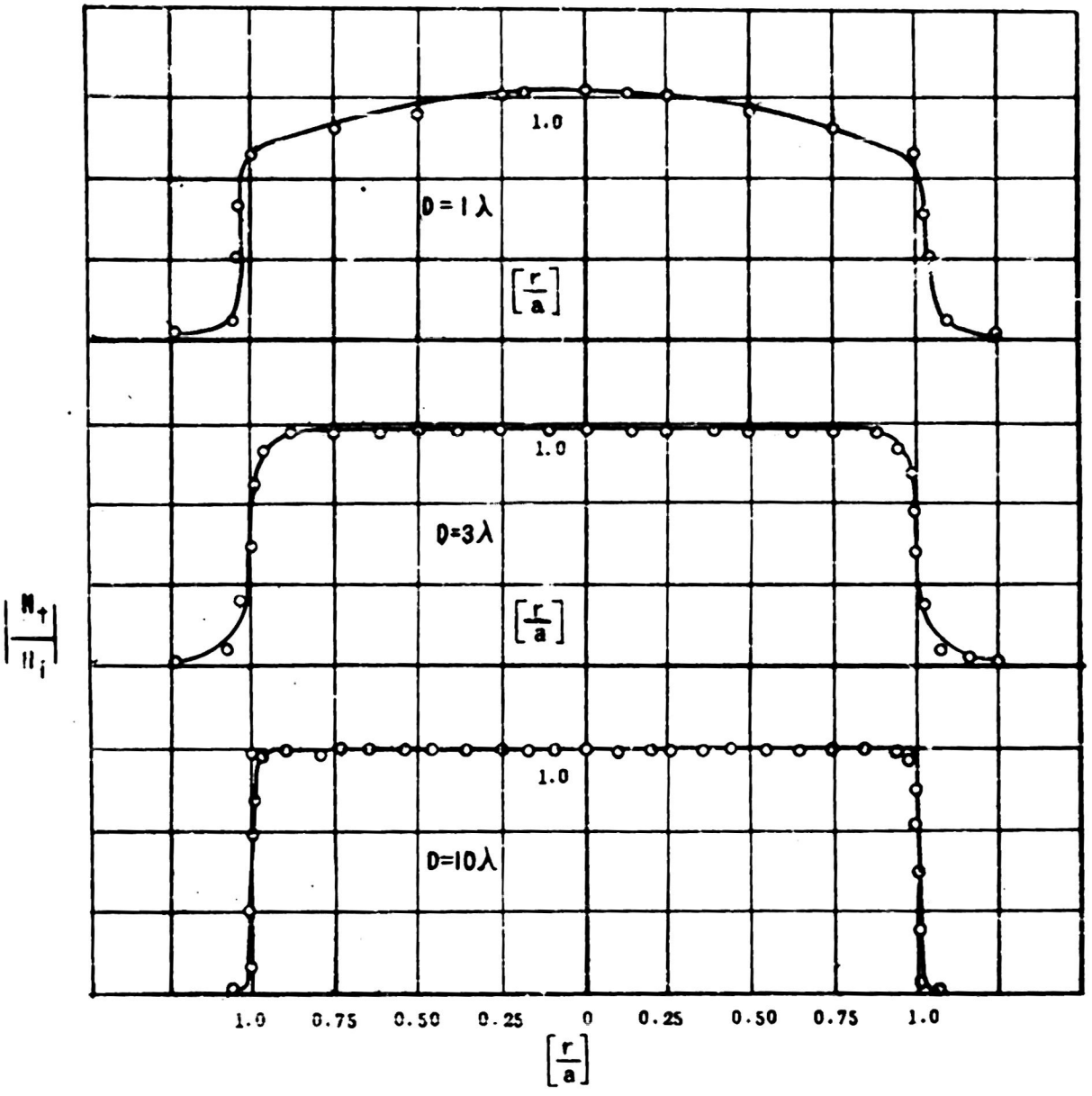

FIG. 10 H_T IN APERTURE PLANE

(1MM BEHIND APERTURE PLANE)

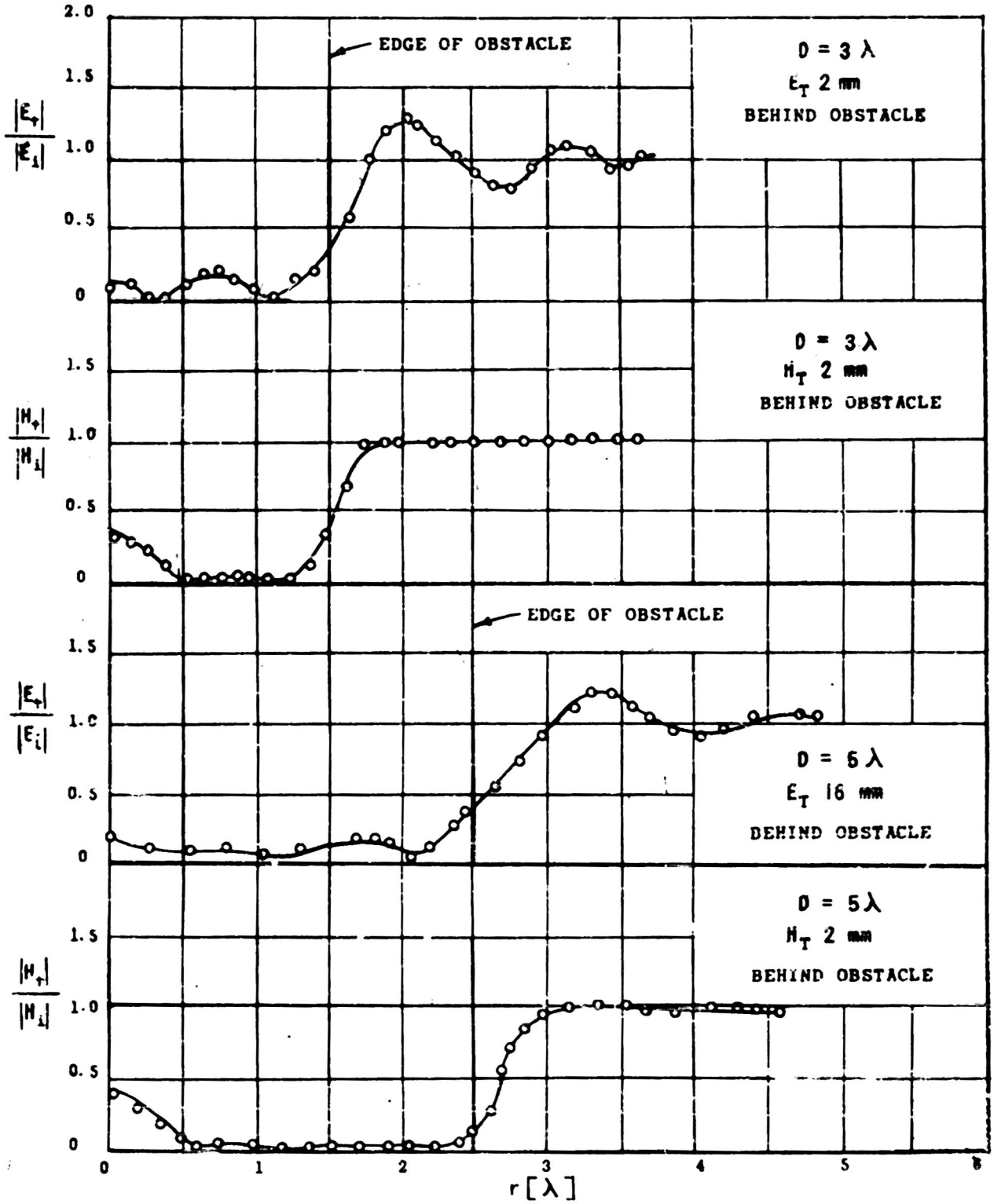

FIG. 11 H_T AND E_T BEHIND OBSTACLE IN H-PLANE

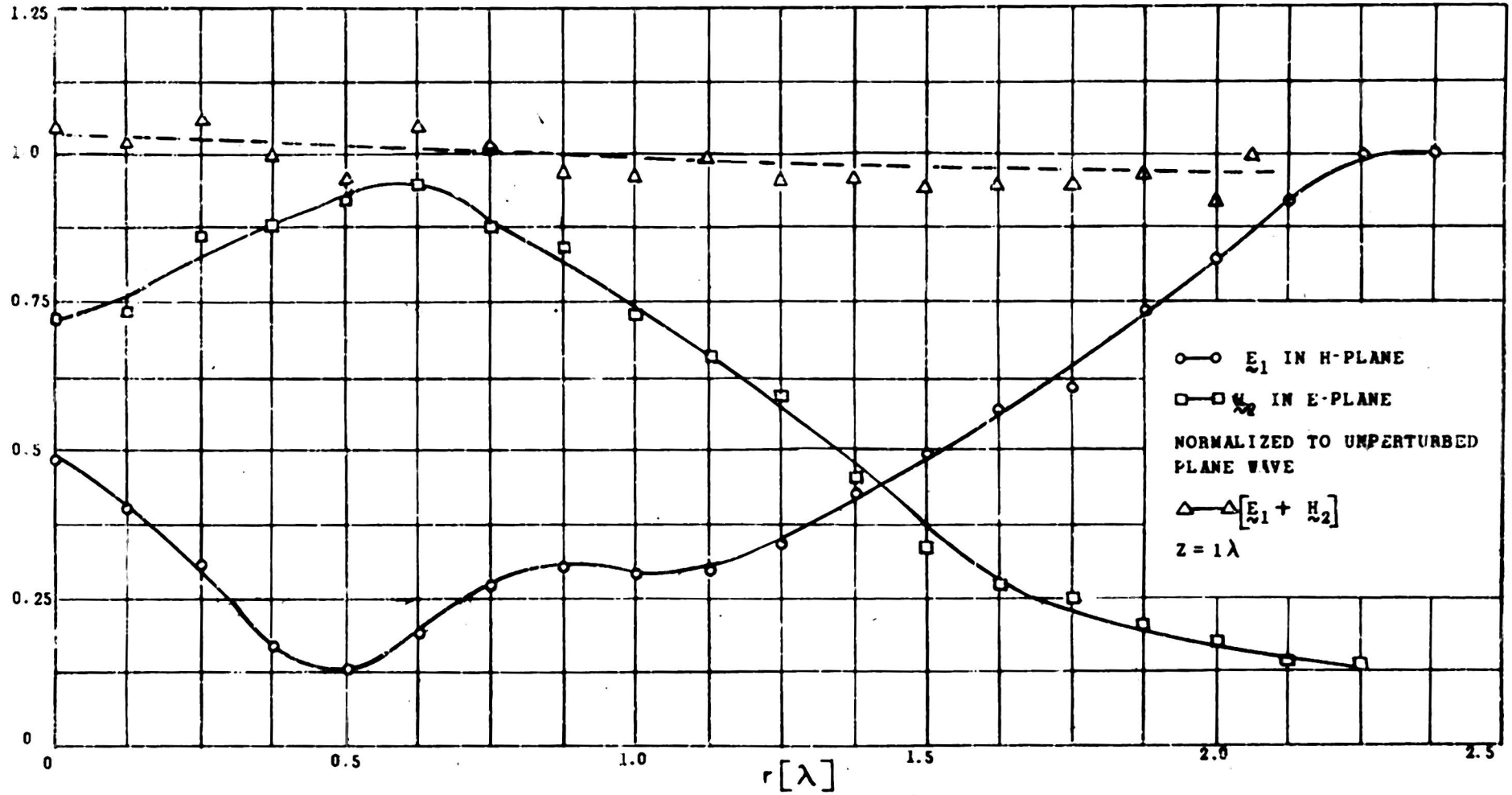

FIG. 12 ELECTROMAGNETIC BABINET PRINCIPLE

[$\underset{\sim}{E}$ AND $\underset{\sim}{H}$ ARE SHOWN IN MAGNITUDE ONLY;
THE ADDITION IS A VECTOR ONE]

$$\hat{E}_1 + \left(\frac{\mu}{\epsilon}\right)^{\frac{1}{2}} \hat{H}_2 = \hat{E}_i$$

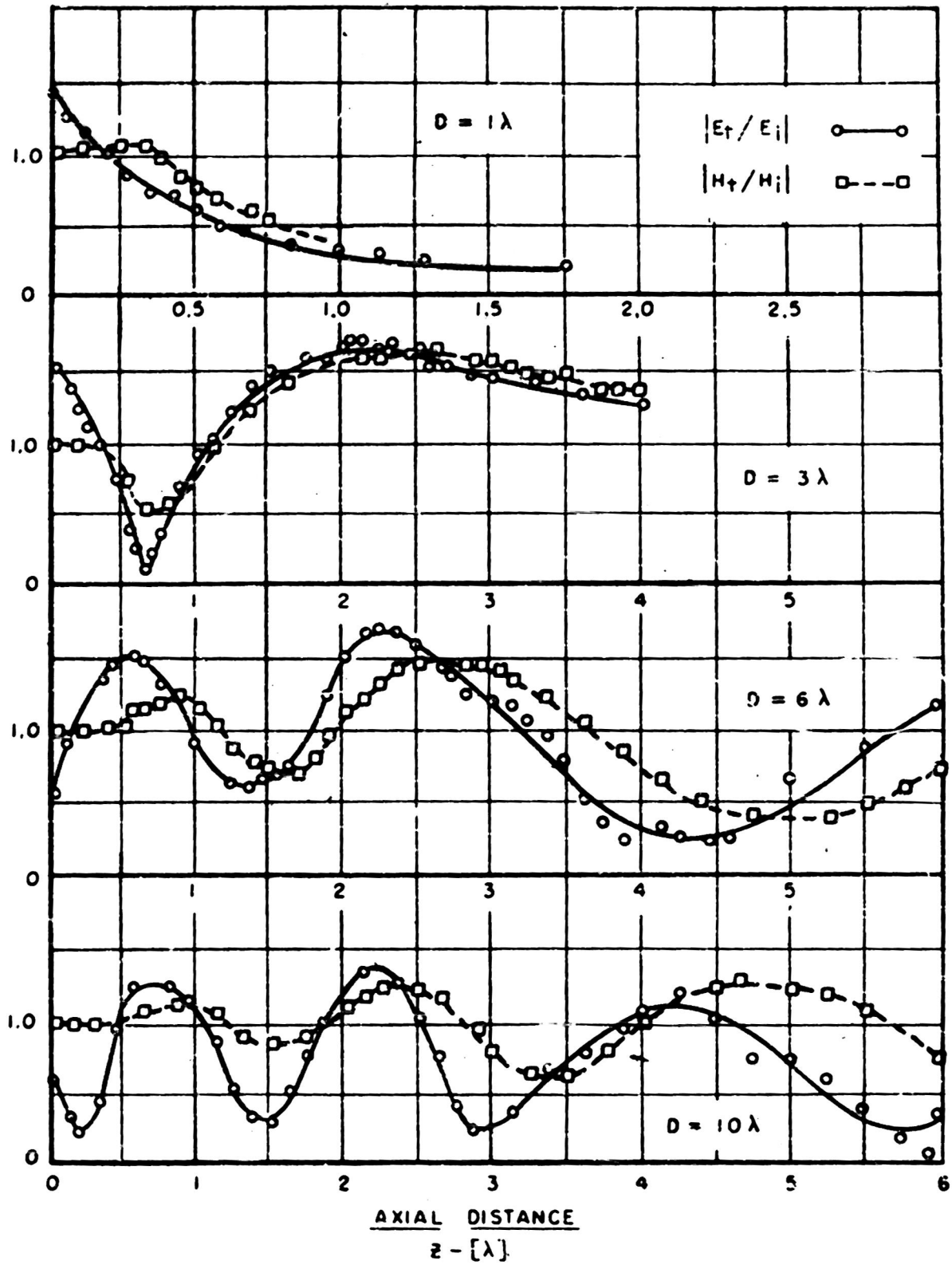

FIG. 13 AXIAL DISTRIBUTIONS

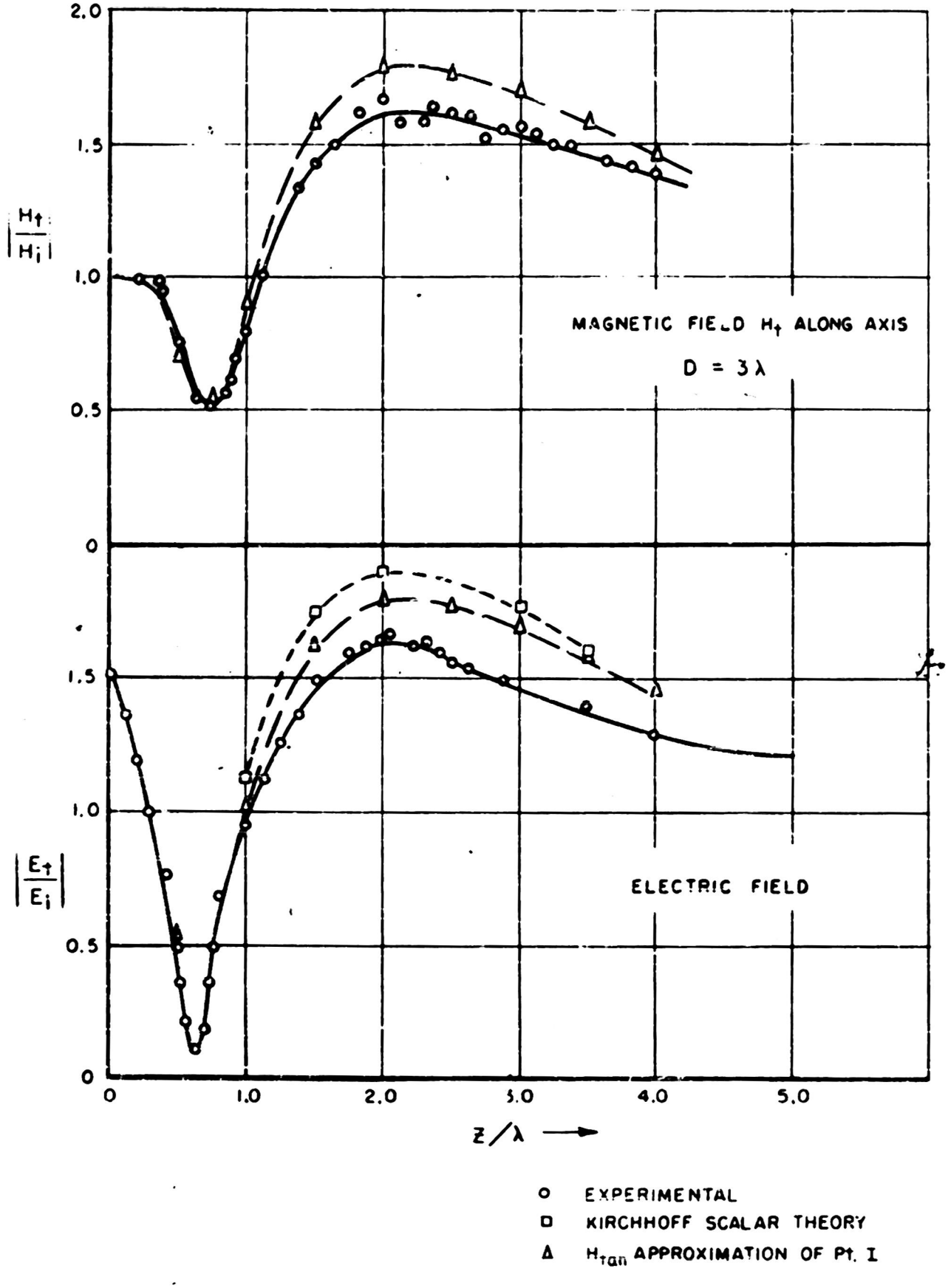

FIG 14 COMPARISON WITH THEORY– AXIAL DISTRIBUTIONS

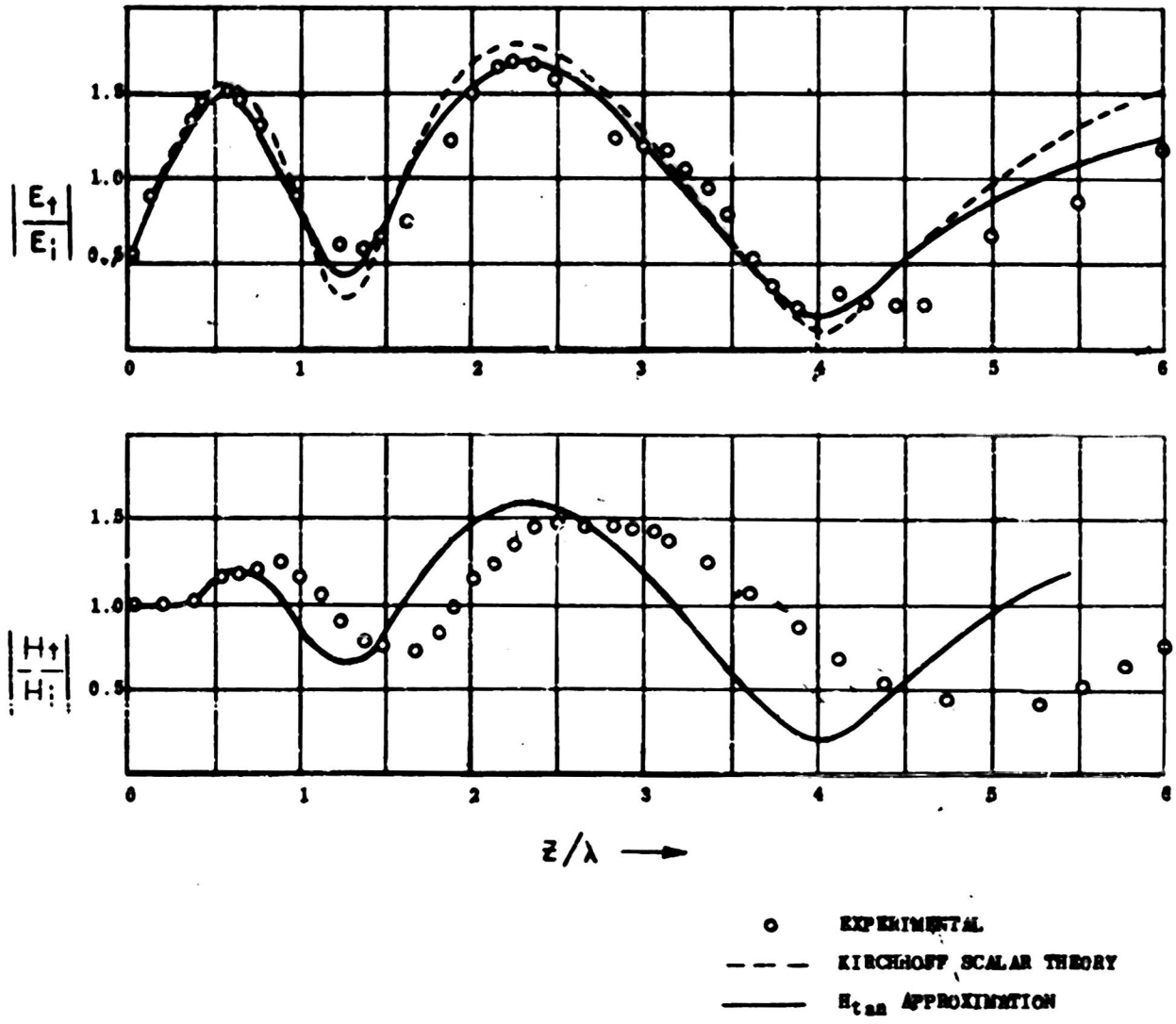

FIG. 15 COMPARISON WITH THEORY — AXIAL DISTRIBUTIONS

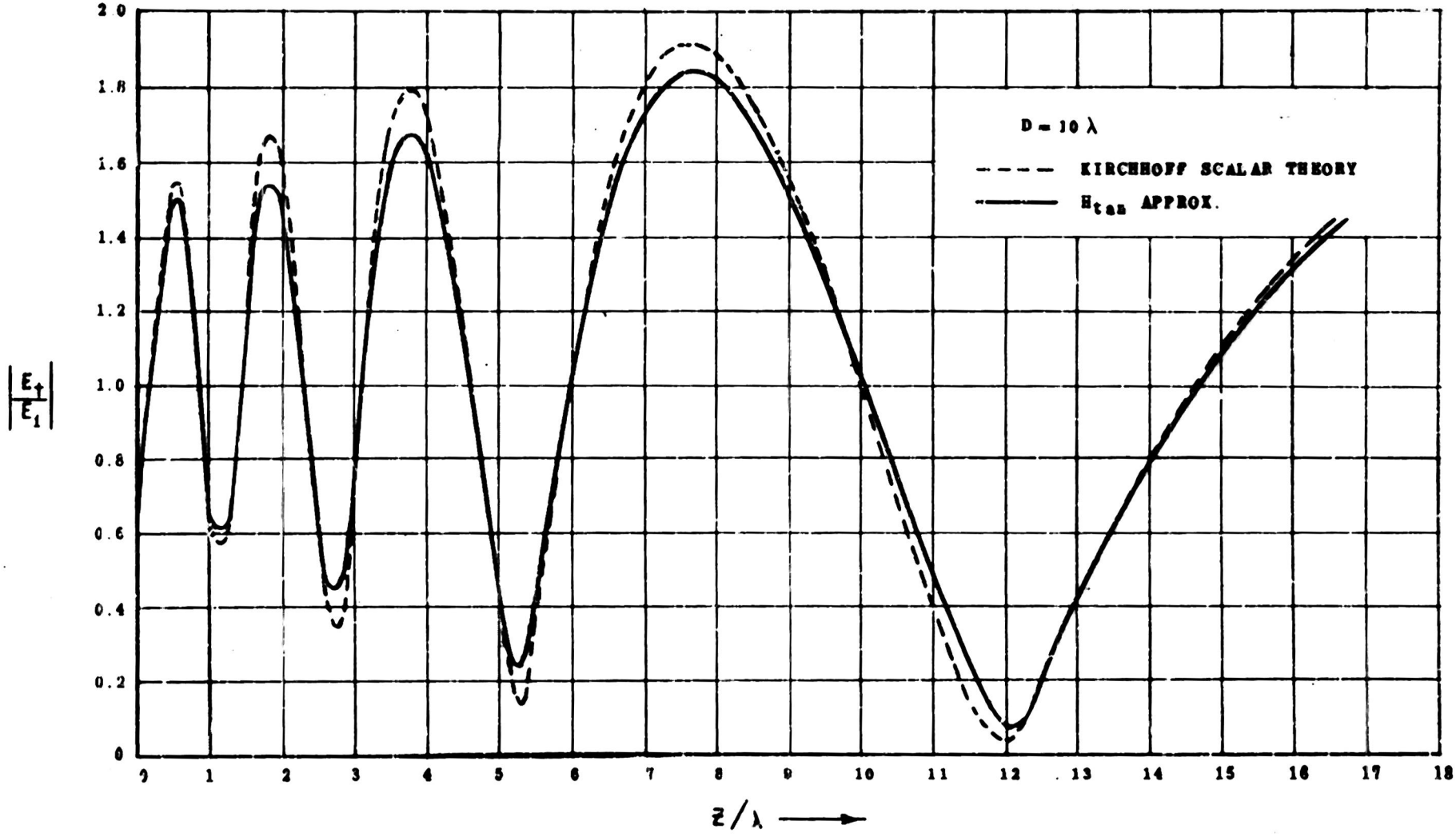

FIG. 16 COMPARISON OF KIRCHHOFF THEORY WITH H_{tan} APPROXIMATION; AXIAL DISTRIBUTION

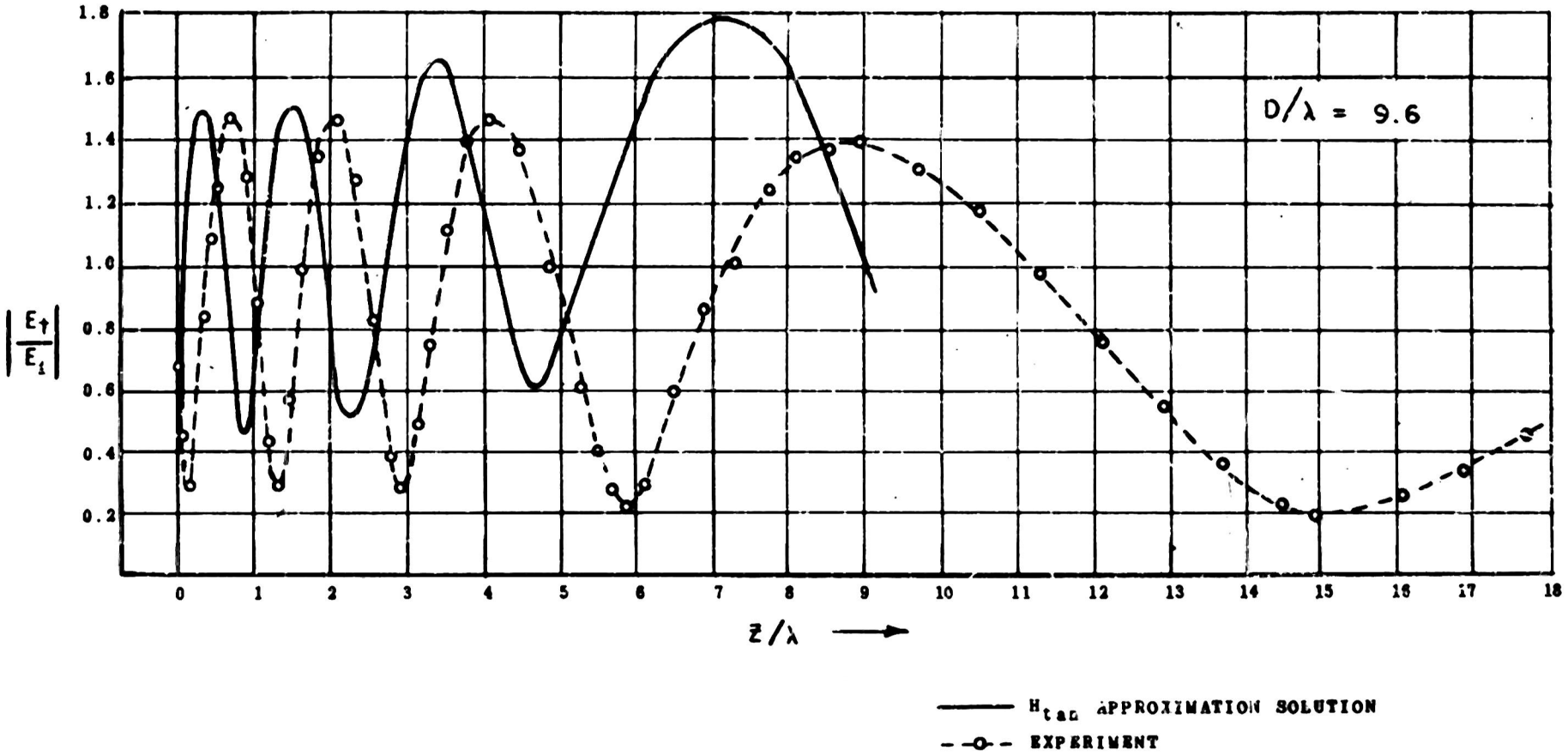

FIG. 17 AXIAL DISTRIBUTION OF E_{tan}

BIBLIOGRAPHY

1. Andrews, C. L., Physics Review, 71, 777 (1947); Journal of Applied Physics, 21, 761 (1950)

2. Baker and Copson, Mathematical Theory of Huygen's Principle (Oxford Press 1939)

3. Booker, H., Journal of Institute of Electrical Engineers, 93, Pt. IIIA, No. 4, 620 (1946)

4. Bouwkamp, C.J., Philips Research Report 5, 321-332, 401-422 (1950)

5. Bouwkamp, C.J., Physica, 12, 467 (1946)

6. Meixner, J., Ann. d. Physik, 6, 1 (1949); also Vol. 7 (1950)

7. Severin, H., Zuts f. Naturforsch 1, 487 (1946)

8. Silver, S. and Ehrlich, M.J., Diffraction of a Plane Electromagnetic Wave by a Circular Aperture and Complementary Obstacle Antenna Laboratory Report 181, University of California, Berkeley, December 1951.

9. Sommerfeld, A., Vol II of Frank and U. Mises, Differential und Integralgleichunger der Physik

10. Sterns, W.G., Near-Zone Field Studies of Quasi-Optical Antennas, Antenna Laboratory Report 153, University of California, Berkeley, June, 1949

11. Stratton, J. A., Electromagnetic Theory, Sec. 8.15, (McGraw - Hill Co. 1941)